SUPPORTING INFORMATION

Chinese Journal of Structural Chemistry

Sulfonate-Functionalized Polyoxovanadate-based Metal-Organic Polyhedra for Enhanced Proton Conduction *via* the Synergy of Linker and Metal Cluster Vertex

Yu Zhang[1†], Shan-Shan Liu[1†], Bo Li[2†], Hanqi You[1], Longxi Zhang[1], Zhenyi Zhang[3], Hong-Ying Zang[2*], Qi Zheng[4*] and Weimin Xuan[1*]

[1]*College of Chemistry, Chemical Engineering and Biotechnology & State Key Laboratory for Modification of Chemical Fibers and Polymer Materials, Donghua University, Shanghai 201620, China*

[2]*Key Laboratory of Polyoxometalate and Reticular Material Chemistry of Ministry of Education at Universities of Jilin Province, Faculty of Chemistry, Northeast Normal University, Changchun 130024, China*

[3]*Bruker (Beijing) Scientific Technology Co., Ltd 9F, Building No.1, Lane 2570, Hechuan Rd, Minhang District, Shanghai 200233, China*

[4]*State Key Laboratory for Modification of Chemical Fibers and Polymer Materials, College of Materials Science and Engineering, Donghua University, Shanghai 201620, China*

**Corresponding authors. Emails: weiminxuan@dhu.edu.cn, qi.zheng@dhu.edu.cn and zanghy100@nenu.edu.cn*

TABLE OF CONTENTS

SUPPORTING INFORMATION

Chinese Journal of Structural Chemistry

n MATERIALS

The solid drugs and solvents used in the experiment are commercial reagents, and no additional purification is required.

n INSTRUMENTATION

Crystallography. X-ray diffraction details for **1-2**: The data were collected on a Bruker/ARINAX MD2 diffractometer equipped with a MarCCD-300 detector at beam line station BL17B of Shanghai Synchrotron Radiation Facility (SSRF). Suitable single crystal was mounted on a Nylon loop with Paratone-N oil for diffraction at 100 K. All experiments were conducted by using the radiation with wavelengths of 0.68873 and 0.67011 Å (E = 19 keV), and the detector distance was 90 mm. For each dataset, 360 frames were collected by using ω-scans with an oscillation range of 1° and an exposure time of 1 s. Data collection was performed using the BlueIce software package. Cell refinements, data reductions and absorption corrections were carried out using the HKL3000 and Apex3 software package. All structures were solved by direct methods and refined by full-matrix least-squares on F^2 using SHELXTL software. Non-hydrogen atoms were refined with anisotropic displacement parameters. Hydrogen atoms were calculated in ideal positions with isotropic displacement parameters set to $1.2U_{eq}$ or $1.5U_{eq}$ of the attached atoms. Contributions of highly disordered solvents were removed by SQUEEZE routine using PLATON.[1] DISP instruction was used for all datasets. Crystallographic data have been deposited at the Cambridge Crystallographic Data Centre (CCDC) under CCDC numbers: 2156151 and 2156152.

Powder X-ray Diffraction (PXRD). Powder XRD was recorded on a Haoyuan DX-2700B diffractometer equipped with monochromatized Cu-Kα (λ = 1.5418 Å) radiation in the range of 2 ≤ 2θ≤ 45° with a scanning rate of 4 °·s^{-1}.

Thermogravimetric Analysis (TGA). Thermogravimetric Analysis (TGA) was conducted on a PerkinElmer TGA 8000 Thermogravimetric Analyzer from 50 to 800 ºC under N_2 at a rate of 10 ºC·min^{-1}.

Fourier-transform Infrared (FT-IR) Spectroscopy. The samples were prepared as a KBr pellet and the FT-IR spectrum was collected in transmission mode in the range of 500-4000 cm^{-1} using a NEXUS-670 spectrometer. Wavenumbers are given in cm^{-1}. Intensities are denoted as w = weak, m = medium, s = strong, br = broad.

Element Analyses. The contents of C, H and N elements are determined by the VarioEL III Elemental Analyzer.

Method of Proton Conduction Testing. The AC impedance test is performed at the IviumStat electrochemical workstation CHR 604E, with a frequency range of 0.01-10^5 Hz and an AC voltage of 50 mV, to test the proton conductivity of **2** and **3**. As a result of the impedance data being equivalent to the ZSimpWin software, a Nyquist graph can be generated. Measurements were performed at: (1) 30 °C and various humidities (60%-90% RH); (2) 90% RH and various temperatures (30-65 °C). The proton conductivity was calculated using the following equation.

$$\sigma = \frac{L}{SR}$$

where σ is the ion conductivity, L is the thickness, R is the resistance of the pellet, and S is the area of the pellet. Activation energy (Ea) can be calculated using the formula.

$$\sigma T = \sigma_0 \exp(-E_a/k_B T)$$

where σ_0 is the pre-exponential factor, k_B is the Boltzmann constant, and T is the temperature.

n SYNTHETIC PROCEDURE OF 1-3

1: $(NMe_4)_x(NHMe_3)_{14-x}[Na_6(V_5O_9Cl)_4(L)_8Cl_4(C_2H_4N_4)_4]$, M.W.: 4861.11

VCl_3 (0.06 g, 0.382 mmol), 5-sulfoisophthalic acid monosodium salt (0.025 g, 0.093 mmol) and 4-amino-1,2,4-triazole (0.008 g, 0.093 mmol) were added to DMF (2 mL), MeOH (0.5 mL) mixed solution, and then the mixture was sealed in a 10 mL Parr Teflon-lined stainless steel vessel at 130 °C for 3 days. After slowly cooling to room temperature, the dark green block crystals were obtained and washed with MeOH (yield: 33%. based on ligand). Due to poor repeatability, compound **1** was not characterized by XRD, TGA, IR and EA.

2: $(NH_2Me_2)_{12}[(V_5O_9Cl)_6(L)_8]\cdot 11CH_3OH\cdot 12DMF$, M.W.: 5015.08

VCl_3 (0.03 g, 0.19 mmol), 5-sulfoisophthalic acid monosodium salt (0.0125 g, 0.047 mmol) and $Li_2B_4O_7$ (0.013 g, 0.075 mmol) were added to DMF (1 mL), MeOH (0.25 mL) mixed solution, and then the mixture was sealed in a 10 mL Parr Teflon-lined stainless steel vessel at 130 °C for 3 days. After slowly cooling to room temperature, the dark green block crystals were obtained and washed with DMF (yield: 68%. based on ligand). ICP analysis, calc.: V: 24.89%; Cl: 3.47%; found: V: 24.92%; Cl: 3.51%. Elemental analysis, calc.: C, 26.70%; H, 4.22%; N, 4.29%; found: C, 26.77%; H, 4.23%; N, 4.31%. IR (KBr, cm^{-1}): 3435(br), 2926(w), 1608(s), 1564(s), 1487(s), 1448(s), 1391(s), 1201(m), 1111(w), 1048(w), 1007(m), 986(s), 949(w), 772(w), 720(w), 631(s), 593(w), 529(w), 497(w).

3: $(NH_2Me_2)_{12}[(V_5O_9Cl)_6(C_9H_3O_6)_8]$, M.W.: 4814.93

A mixture of H_3BTC (0.025 g, 0.12 mmol) and $VOCl_3$ (0.1 mL) was dissolved in a mixed solvent of DMF (2 mL) and CH_3OH (0.5 mL) with stirring for 30 min, and then sealed in a 15 mL Parr Teflon-lined stainless steel vessel. The mixture was heated at 160 °C for 2d under autogenous pressure

and then gradually cooled to room temperature. Dark-green block-shaped crystals suitable for X-ray analysis were obtained by washing with methanol and drying at room temperature (65% yield, based on H_3BTC). ICP analysis, calc.: V: 31.74% Cl: 4.42%; found: V: 31.70%; Cl: 4.45%. Elemental analysis, calc.: C, 23.95%, H, 2.51%, N, 3.49%; found: C, 23.77%, H, 2.35%, N, 3.72%. IR (KBr, cm^{-1}): 3411 (br), 3033 (w), 2925 (w), 1668 (w), 1617 (s), 1566 (s), 1486 (m), 1447 (s), 1389 (vs), 1108 (m), 1006 (m), 986 (m), 948 (w), 755 (s), 721 (s), 637 (s), 586 (m), 528 (m), 499 (m).

n CRYSTALLOGRAPHIC DATA AND CRYSTAL STRUCTURES OF 1-2

Table S1. Crystallographic Details for Compounds **1** and **2**

Compound	**1**	**2**
empirical formula	$C_{102}H_{130}Cl_8N_{24}Na_6O_{92}S_8V_{20}$	$C_{83}H_{100}Cl_6N_8O_{113}S_8V_{30}$
formula weight	4861.11	5015.08
temperature (K)	100(2)	100(2)
crystal system	monoclinic	cubic
space group	*C*2/c	$Fm\bar{3}$
unit cell dimention	a = 23.4497(5) Å, α = 90°	a = 29.6244(17) Å, α = 90°
	b = 35.5201(7) Å, β = 102.1140(10)°	b = 29.6244(17) Å, β = 90°
	c = 31.0285(9) Å, γ = 90°	c = 29.6244(17) Å, γ = 90°
volume ($Å^3$)	25269.2(10)	25999(4)
Z	4	4
density (calculated) (Mg/m^3)	1.278	1.281
absorption coefficient (mm^{-1})	0.850	1.025
F(000)	9744	9912
reflectionscollected/unique	196988	74465
data/restraints/parameters	28902/3852/1596	2119/1316/359
goodness-of-fit on F^2	1.022	1.288
final R indices [I>2δ (I)]	R1 = 0.0565, wR2 = 0.1545	R1 = 0.1029, wR2 = 0.2794
R indices (all data)	R1 = 0.0629, wR2 = 0.1601	R1 = 0.1091, wR2 = 0.2836
largest diff. peak and hole (e. $Å^{-3}$)	1.243 and -1.563	1.278 and -0.959

n SELECTED BOND LENGTHS FOR 1 AND 2

Table S2. Selected Bond Lengths for Compound **1**

Bond	Length	Bond	Length
V(1)-O(2)	1.965(4)	V(6)-O(8)	1.882(4)
V(1)-O(3)	1.592(5)	V(6)-O(9)	1.881(5)
V(1)-O(4)	1.936(4)	V(7)-O(8)	1.974(5)
V(1)-O21	2.008(4)	V(7)-O(9)	1.957(4)
V(1)-O26	2.014(4)	V(7)-O(13)	1.602(5)
V(2)-O(2)#1	1.971(4)	V(7)-O31	1.999(4)
V(2)-O(4)	1.972(4)	V(7)-O36	2.010(5)
V(2)-O(5)	1.595(4)	V(8)-O(7)	1.958(4)
V(2)-O11#1	2.014(4)	V(8)-O(9)	1.957(4)
V(2)-O16	2.012(4)	V(8)-O(12)	1.594(4)
V(3)-O(2)#1	1.881(4)	V(8)-O13	2.012(4)
V(3)-O(2)	1.881(4)	V(8)-O46	2.018(5)
V(3)-O(4)	1.882(4)	V(9)-O(14)	1.598(4)
V(3)-O(4)#1	1.882(4)	V(9)-O(17)	1.953(4)
V(3)-O(19)	1.602(6)	V(9)-O(18)	1.959(4)
V(4)-O(6)	1.965(4)	V(9)-O43	2.013(4)
V(4)-O(8)	1.949(5)	V(9)-O15#1	2.005(9)
V(4)-O(10)	1.598(5)	V(10)-O(15)	1.605(7)
V(4)-O41	2.021(4)	V(10)-O(17)#1	1.889(4)
V(4)-O44	2.003(5)	V(10)-O(17)	1.889(4)
V(5)-O(6)	1.967(4)	V(10)-O(18)	1.883(5)
V(5)-O(7)	1.954(4)	V(10)-O(18)#1	1.883(5)
V(5)-O(11)	1.597(4)	V(11)-O(16)	1.600(5)
V(5)-O23	2.009(4)	V(11)-O(17)#1	1.954(4)
V(5)-O34	2.005(5)	V(11)-O(18)	1.956(4)
V(6)-O(01N)	1.603(5)	V(11)-O33#1	2.010(4)
V(6)-O(6)	1.864(5)	V(11)-O25#1	2.005(9)
V(6)-O(7)	1.882(4)		

Table S3. Selected Bond Lengths for Compound **2**

Bond	Length	Bond	Length
V(1)-O(1)#1	2.037(7)	V(2)-O(11)#1	1.874(8)
V(1)-O(2)	1.987(8)	V(2)-O(11)	1.874(8)
V(1)-O(4)	1.580(6)	V(3)-O(2)#1	1.988(8)
V(1)-O(9)	1.970(7)	V(3)-O(3)	1.958(8)
V(1)-O(11)	1.933(8)	V(3)-O(7)	1.587(6)
V(2)-O(2)#1	1.891(8)	V(3)-O(10)	2.041(7)
V(2)-O(2)	1.891(8)	V(3)-O(11)	1.954(7)
V(2)-O(8)	1.632(9)		

n BOND VALENCE SUM (BVS) CALCULATIONS OF V ATOMS IN 1 AND 2

Table S4. Bond Valence Sum (BVS) Calculations of V Atoms in Compound **1**

Compound 1	BVS calc. for V (IV)	BVS calc. for V (V)
V1	4.032	4.290
V2	3.945	4.198
V3	4.659	4.958
V4	3.990	4.246
V5	3.992	4.248
V6	4.689	4.989
V7	3.965	4.219
V8	3.984	4.240
V9	3.994	4.251
V10	4.613	4.908
V11	3.997	4.253

Table S5. Bond Valence Sum (BVS) Calculations of V Atoms in Compound **2**

Compound 2	BVS calc. for V (IV)	BVS calc. for V (V)
V1	4.086	4.348
V2	4.526	4.816
V3	4.029	4.288

n COORDINATION PATTERNS OF SODIUM ATOMS IN 1 AND PACKING STRUCTURE OF 1

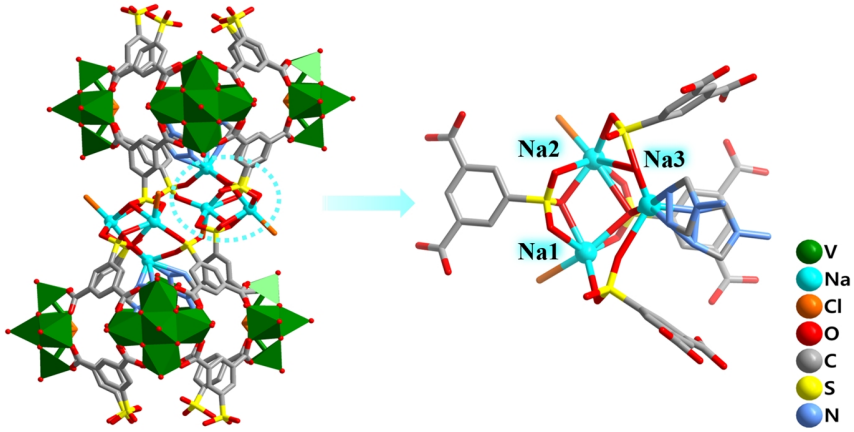

Figure S1. Coordination patterns of sodium atoms in **1**. H atoms are omitted for clarity.

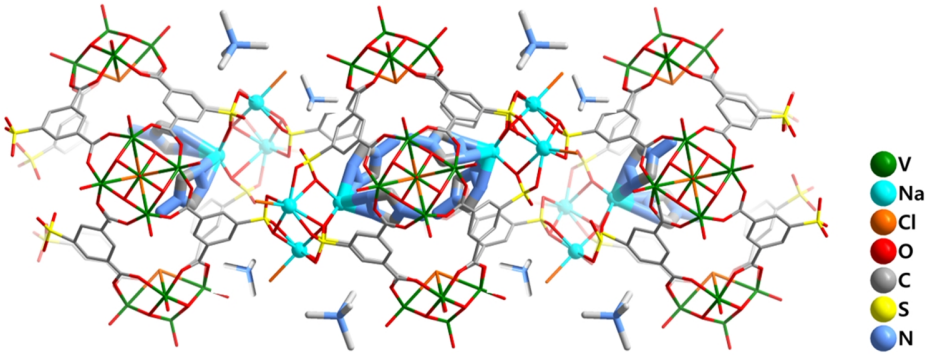

Figure S2. Packing structure of **1**. The counterions include $[NMe_4]^+$ and $[NHMe_3]^+$. H atoms are omitted for clarity.

n XPS SPECTRA OF 2

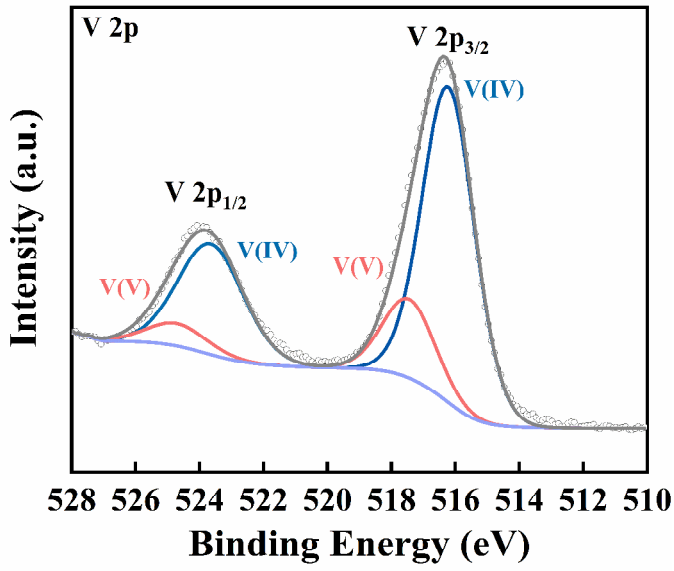

Figure S3. XPS spectra of **2**.

n PACKING STRUCTURE OF 2

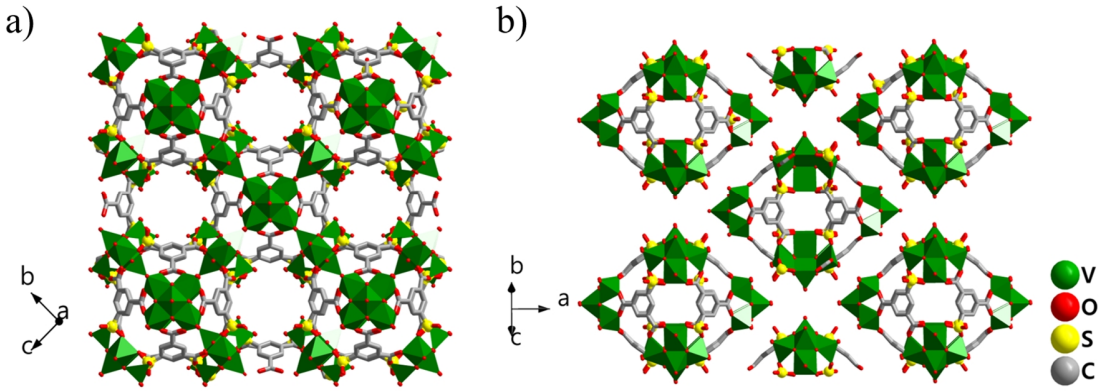

Figure S4. Structures of **2** with view in different directions. H atoms are omitted for clarity.

n PACKING STRUCTURE OF 3

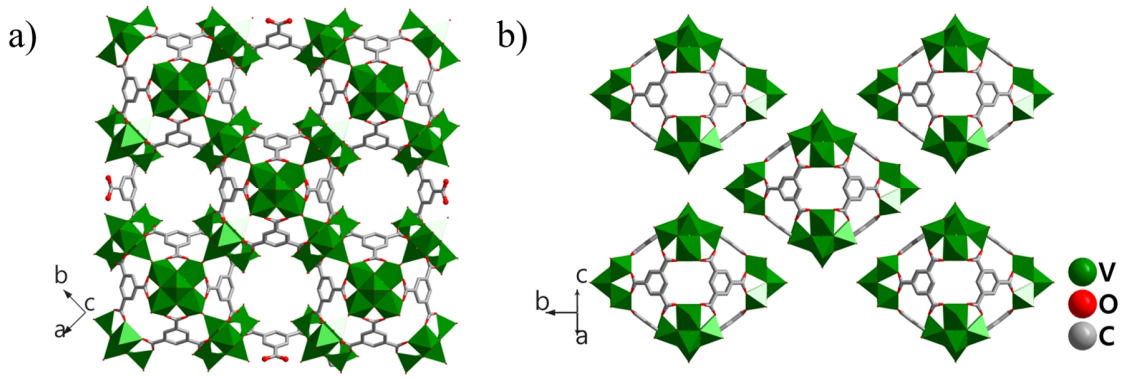

Figure S5. Structures of **3** with view in different directions. H atoms are omitted for clarity.

n PXRD PATTERN OF 2

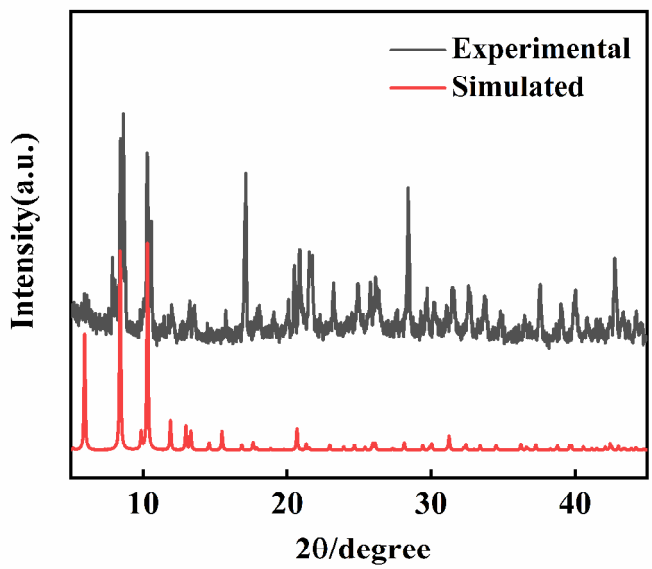

Figure S6. Experimental and simulated PXRD patterns of **2**.

n TGA CURVE OF 2

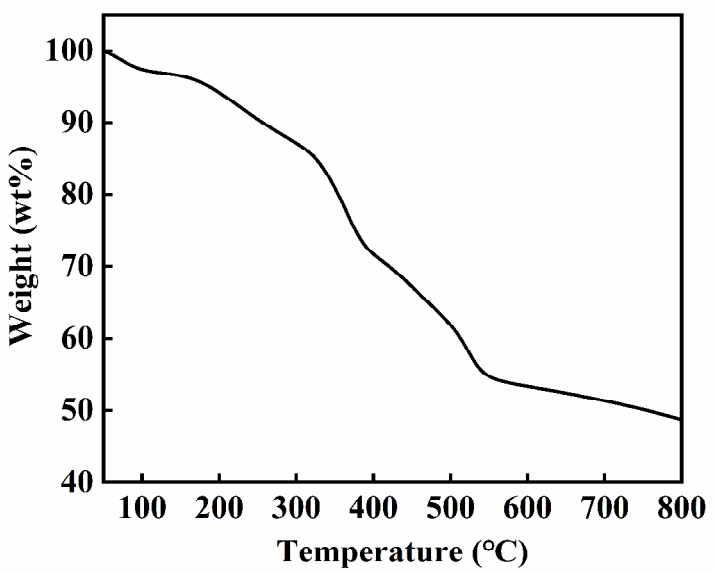

Figure S7. TGA curve of **2**.

n IR SPECTRUM OF 2

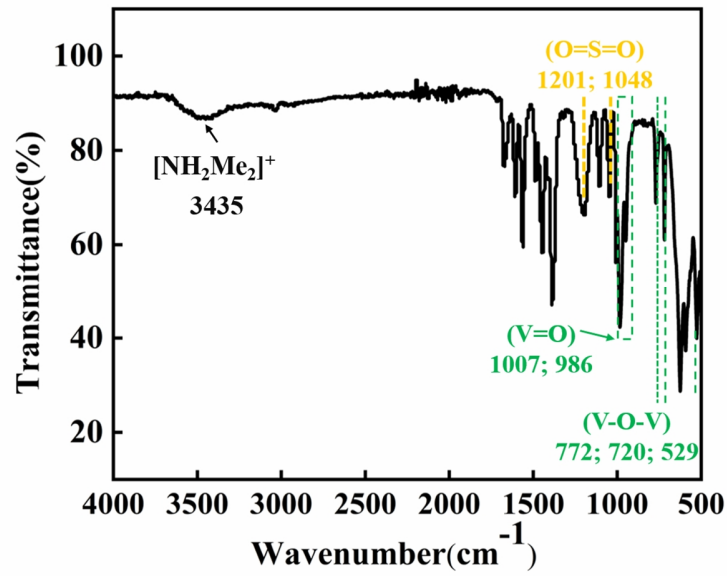

Figure S8. The IR spectrum of **2**.

n PROTON CONDUCTION RESULTS OF 2

Table S6. Resistance (R) and Proton Conductivity (σ) of **2** under Different Relative Humidities and 30 ℃

RH (%)	R (Ω)	σ (S cm^{-1})
60	3.70×10^{6}	1.29×10^{-7}
70	1.56×10^{5}	3.06×10^{-6}
80	3.04×10^{3}	1.57×10^{-4}
90	8.80×10^{1}	5.43×10^{-3}

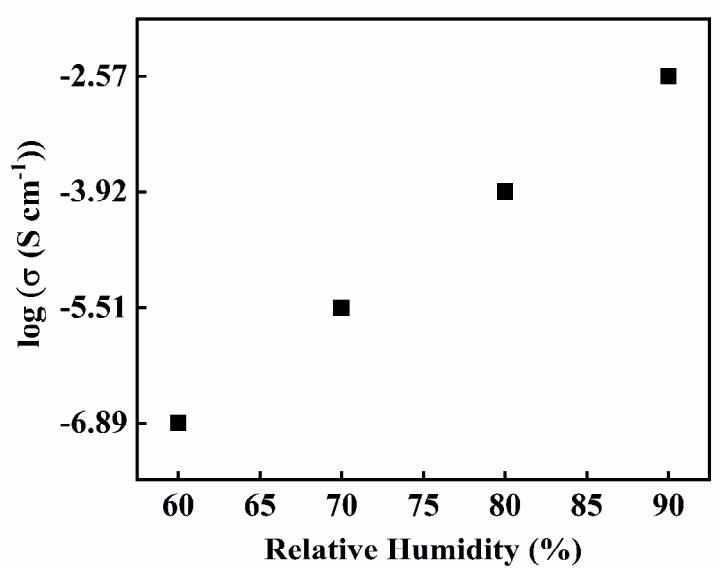

Figure S9. The scatter plot of the relationship between proton conductivity of compound **2** and different humidities at 30 °C.

Table S7. Proton Conductivity (σ) of **2** under Different Temperature and 80% RH

Temperature (℃)	Proton conductivity (S cm^{-1})	Temperature (℃)	Proton conductivity (S cm^{-1})
30	1.57×10^{-4}	50	6.04×10^{-4}
35	2.85×10^{-4}	55	7.15×10^{-4}
40	4.61×10^{-4}	60	7.73×10^{-4}
45	5.75×10^{-4}	65	8.73×10^{-4}

Table S8. Proton Conductivity (σ) of **2** under Different Temperatures and 90% RH

Temperature (℃)	Proton conductivity (S cm^{-1})	Temperature (℃)	Proton conductivity (S cm^{-1})
30	5.43×10^{-3}	50	1.54×10^{-2}
35	6.96×10^{-3}	55	2.04×10^{-2}
40	8.23×10^{-3}	60	2.71×10^{-2}
45	1.13×10^{-2}	65	3.02×10^{-2}

n WATER ADSORPTION-DESORPTION ISOTHERMS OF 2

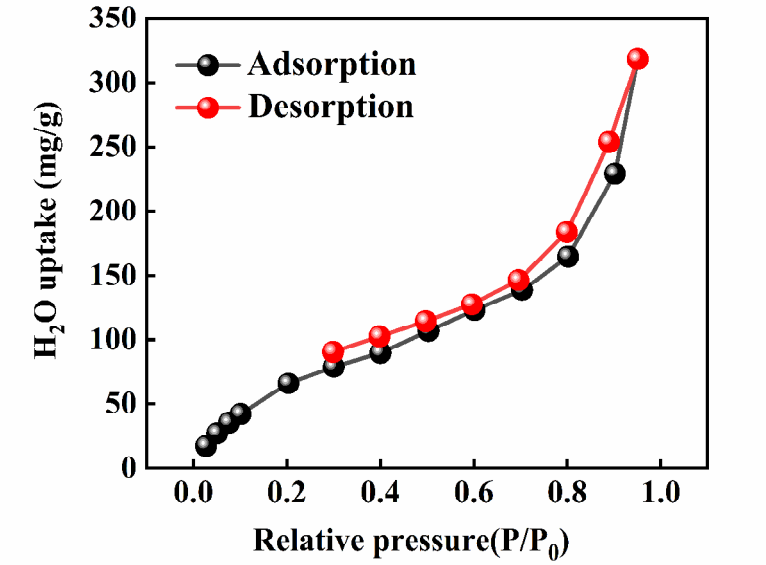

Figure S10. Water vapor sorption isotherms of **2**.

n PROTON CONDUCTION RESULTS OF 3

Table S9. Proton Conductivity (σ) of Compound **3** under Different Temperatures and 90% RH

Temperature (℃)	Proton conductivity (S cm^{-1})	Temperature (℃)	Proton conductivity (S cm^{-1})
30	2.23×10^{-3}	50	3.29×10^{-3}
35	2.60×10^{-3}	55	3.57×10^{-3}
40	2.82×10^{-3}	60	3.88×10^{-3}
45	3.02×10^{-3}	65	4.27×10^{-3}

n PROTON CONDUCTIVITY OF THE REPORTED MOPS

Table S10. Proton Conductivity of the Reported MOPs.

Material (powder)	Metal/metal cluster node	Proton conduction channel	Proton conductivity (S cm^{-1})	RH, %	T, ℃	Reference
$(NH_2Me_2)_{12}[(V_5O_9Cl)_6(L)_8]$	$\{V_5\}$	3D	3.02×10^{-2}	90	65	This work
$[Co_{16}(TPC4R\text{-}I)_2(HL)_4(L)_8(H_2O)_{24}$ (1-SO_3H)	$\{Co_4\}$	1D	1.35×10^{-2}	98	90	[2]
$[Cp_3Zr_3(\mu_3\text{-}O)(\mu_2\text{-}OH)_3]_2L_3$	$\{Zr_3\}$	2D	1.41×10^{-3}	98	30	[3]
$[Mn_6(FeL)_8](ClO_4)_{12}$	{Fe} and {Mn}	3D	3.31×10^{-3}	98	70	[4]
$[Mn_6(CoL)_8](ClO_4)_{12}$	{Co} and {Mn}	3D	1.05×10^{-4}	98	70	
$[Cr_4In_4(Himdc)_{12}]^a$	{Cr} and {In}	3D	5.8×10^{-2}	98	22.5	
$[Cr_4In_4(Himdc)_{12}]^b$	{Cr} and {In}	3D	0.23×10^{-2}	98	22.5	[5]
$[Cr_4In_4(Himdc)_{12}]^c$	{Cr} and {In}	3D	0.65×10^{-2}	98	22.5	
$[Pd_6(Lc)_8(NO_3)_{12}]$	{Pd}	3D	1.1×10^{-3}	98	r.t	[6]

Sample morphology for conductivity measurement: a: single crystal; b: pellet sample at 50 Mpa; c: pellet sample at 68 Mpa.

n COMPARISON OF THE PROTON CONDUCTIVITY OF 2 WITH REPRESENTATIVE POM-BASED PROTON CONDUCTORS

Table S11. Comparison of the Proton Conductivity of **2** with Representative POM-Based Proton Conductors

Material	Proton conductivity (S cm^{-1})	RH, %	T, ℃	Reference
$(NH_4)_{21}H^+_{59-2x}[Mo^V_{180}Mo^{VI}_{60}(OH)_{60}O_{620-x}(SO_3)_{20-x}(SO_4)_x]\cdot ca337H_2O$	1.03×10^{-1}	98	80	[7]
$Na_{16}(NH_4)_{10}H_8\{[W_{14}Ce^{IV}_6O_{61}](W_3Bi_6Ce^{III}_3(H_2O)_3O_{14}][\alpha\text{-}BiW_9O_{33}]_3)_2\}\cdot ca.38H_2O$	2.4×10^{-3}	90	25	[8]
$NaH_{15}\{[P_2W_{15}Nb_3O_{62}]_2(4PBA)_2((4PBA)_2O)\}\cdot 53H_2O$	1.59×10^{-1}	98	90	[9]
$[(CH_3)_4N]_{1.5}K_{5.5}Na_2[I_3\subset(Mo^V_2O_2S_2)_8(Se^{IV}O_3)_8(OH)_8]\cdot 25H_2O$	1.2×10^{-2}	97	55	[10]
$(HIm)_{24}(NH_4)_{20}[Mo_{72}{}^{VI}Mo_{60}{}^{V}O_{372}(CH_3COO)_{30}(H_2O)_{72}]\cdot ca190H_2O$	4.98×10^{-2}	98	60	[11]
$(TEAH)_{14}Na_{10}K_8H_8[(NaP_5W_{30}O_{110})_2\subset Mo_{22}(Fe\text{-}edta)_8O_{68}(H_2O)_2]\cdot 50H_2O$	1.7×10^{-2}	90	95	[12]

n PXRD PATTERNS OF 2 AND 3 AFTER PROTON CONDUCTION

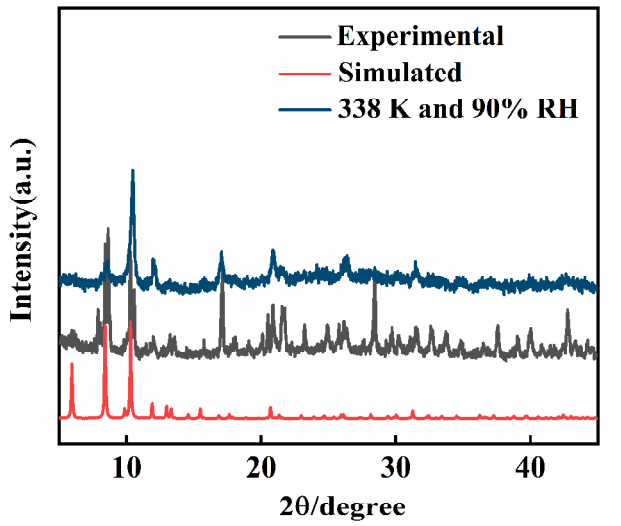

Figure S11. PXRD patterns of compound **2** after proton conduction.

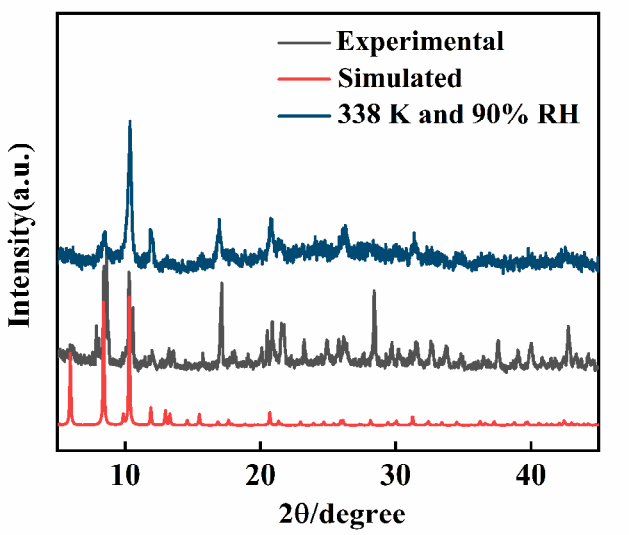

Figure S12. PXRD patterns of compound **3** after proton conduction.

n REFERENCES

(1) Spek, A. L. PLATON SQUEEZE: a tool for the calculation of the disordered solvent contribution to the calculated structure factors. *Acta Crystallogr. C Struct. Chem.* **2015**, 71, 9-18.

(2) Guo, T. T.; Cheng, D. M.; Yang, J.; Xu, X. X.; Ma, J. F. Calix[4]resorcinarene-based [Co_{16}] coordination cages mediated by isomorphous auxiliary ligands for enhanced proton conduction. *Chem. Commun.* **2019**, 55, 6277-6280.

(3) Xing, W. H.; Li, H. Y.; Dong, X. Y.; Zang, S. Q. Robust multifunctional Zr-based metal-organic polyhedra for high proton conductivity and selective CO_2 capture. *J. Mater. Chem. A* **2018**, 6, 7724-7730.

(4) Saha, R.; Samanta, D.; Bhattacharyya, A. J.; Mukherjee, P. S. Stepwise construction of self-assembled heterometallic cages showing high proton conductivity. *Chem. Eur. J.* **2017**, 23, 8980-8986.

(5) Zhai, Q. G.; Mao, C. Y.; Zhao, X.; Lin, Q. P.; Bu, F.; Chen, X. T.; Bu, X. H.; Feng, P. Y. Cooperative crystallization of heterometallic indium-chromium metal-organic polyhedra and their fast proton conductivity. *Angew. Chem. Int. Ed.* **2015**, 54, 7886-7890.

(6) Samanta, D.; Mukherjee, P. S. Component selection in the self-assembly of palladium(II) nanocages and cage-to-cage transformations. *Chem. Eur. J.* **2014**, 20, 12483-12492.

(7) Lin, J. M.; Li, N.; Yang, S. P.; Jia, M. J.; Liu, J.; Li, X. M.; An, L.; Tian, Q. W.; Dong, L. Z.; Lan, Y. Q. Self-assembly of giant Mo_{240} hollow opening dodecahedra. *J. Am. Chem. Soc.* **2020**, 142, 13982-13988.

(8) Liu, J. C.; Han, Q.; Chen, L. J.; Zhao, J. W.; Streb, C.; Song, Y. F. Aggregation of giant cerium-bismuth tungstate clusters into a 3D porous framework with high proton conductivity. *Angew. Chem. Int. Ed.* **2018**, 57, 8416-8420.

(9) Li, S. J.; Zhao, Y.; Knoll, S.; Liu, R. J.; Li, G.; Peng, Q. P.; Qiu, P. T.; He, D. F.; Streb, C.; Chen, X. N. High proton-conductivity in covalently linked polyoxometalate-organoboronic acid-polymers. *Angew. Chem. Int. Ed.* **2021**, 60, 16953-16957.

(10) Zang, H. Y.; Chen, J. J.; Long, D. L.; Cronin L.; Miras, H. N. Assembly of thiometalate-based {Mo_{16}} and {Mo_{36}} composite clusters combining $[Mo_2O_2S_2]^{2+}$ cations and selenite anions. *Adv. Mater.* **2013**, 25, 6245-6249.

(11) Liu, W. J.; Dong, L. Z.; Li, R. H.; Chen, Y. J.; Sun, S. N.; Li, S. L.; Lan, Y. Q. Different protonic species affecting proton conductivity in hollow spherelike polyoxometalates. *ACS Appl. Mater. Interfaces* **2019**, 11, 7030-7036.

(12) Zhu, M. H.; Iwano, T.; Tan, M. J.; Akutsu, D.; Uchida, S.; Chen, G. Y.; Fang, X. K. Macrocyclic polyoxometalates: selective polyanion binding and ultrahigh proton conduction. *Angew. Chem. Int. Ed.* **2022**, 61, e202200666.